MULTIDIMENSIONAL NUMERICAL SIMULATION OF THE REACTING FLOW IN A PULSE COMBUSTOR*

Daniel L. Marcus
Richard B. Pember
John B. Bell
Vincent E. Beckner
Daniel Simkins
Michael Welcome

Lawrence Livermore National Laboratory
Livermore, CA 94551

Abstract

We have developed a new modeling capability to study the behavior of pulse combustors. Our approach is based on the use of higher-order Godunov methods combined with adaptive strategies to focus computational effort where it is required and a Cartesian grid formulation for modeling realistic engineering geometries. The model computes quasi-one-dimensional, axisymmetric, and fully three-dimensional, reacting fluid dynamics in the combustion chamber and incorporates lower-dimensional approximations for both the inlet valve that controls the injection of fuel and the tail pipe whose acoustic properties drive the combustion oscillations.

Introduction

Combustion systems that take advantage of a periodic combustion process have many advantages over conventional systems. Their rate of heat transfer is greatly enhanced and their pollutant emissions are lower. They draw in their own supply of fuel and air and they are self-venting. They have few moving parts.

The most common type of pulse combustor is based on a Helmholtz resonator – a burning cycle drives a resonant pressure wave, which in turn enhances the rate of combustion, resulting in a self-sustaining, large-scale oscillation. Although the basic physical mechanisms controlling such a process were explained by Rayleigh over a century ago, a full understanding of the operation of a pulse combustor still

*This work was performed under the auspices of the U.S. Department of Energy by the Lawrence Livermore National Laboratory under contract W-7405-Eng-48. Support under contract W-7405-Eng-48 was provided by the Applied Mathematical Sciences Program and the HPCC Grand Challenge Program of the Office of Scientific Computing at DOE.

does not exist. The dominant processes in such a system – combustion, turbulent fluid dynamics, acoustics – are highly coupled and interact nonlinearly, which has reduced the design process to a costly and inefficient trial-and-error procedure.

Several recent numerical and experimental studies, however, have been focused towards a better understanding of the basic underlying physics. Barr *et al.* (1990) have elucidated the relative roles of the time scales governing the energy release, the turbulent mixing, and the acoustics. Keller *et al.* (1989) have demonstrated the importance of the phase relation between the resonant pressure field in the tailpipe and the periodic energy release.

In this study, we carry out quasi-one-dimensional, axisymmetric, and three-dimensional simulations of a pulse combustor. The quasi-one-dimensional simulations provide a relatively inexpensive means of exploring the long-term ($> 50,000$ time steps) behavior of the system. We employ a fully conservative seond-order Godunov algorithm for the inviscid, reacting gas dynamics equations coupled to an adaptive mesh refinement procedure (Berger and Colella, 1989). The axisymmetric and three-dimensional simulations allow us to explore in detail the interaction between the transient fluid dynamics phenomena and the energy release associated with the combustion. For these simulations, we couple a second-order, unsplit Godunov algorithm for the inviscid, reacting gas dynamics equations to an adaptive Cartesian grid scheme (Pember *et al*, 1993).

In order to keep computational costs relatively low, we have developed a "bootstrap" procedure to initialize progressively higher-dimensional calculations. The quasi-one-dimensional code is run until transient phenomena have subsided and a desirable quasi-steady state has been achieved. The state data is then extrapolated to axisymmetric coordinates and these conditions used to initialize an axisymmetric calculation. The axisymmetric code is then run through several full combustion cycles and the data mapped to initialize a three-dimensional calculation.

Governing Equations and Numerical Method

We solve the inviscid, compressible Euler equations for reacting flow. Two addional conservation equations are needed for the kinetics (described in the next section). For the purposes of exposition, we write the equations in three-dimensional, Cartesian coordinates. They are, in conservation form:

$$\frac{\partial U}{\partial t} + \frac{\partial F^x}{\partial x} + \frac{\partial F^y}{\partial y} + \frac{\partial F^z}{\partial z} = S \tag{1}$$

where

$$U = \begin{pmatrix} \rho \\ \rho u \\ \rho v \\ \rho w \\ \rho E \\ \rho z \\ \rho \tau \end{pmatrix}$$

$$F^x = \begin{pmatrix} \rho u \\ \rho u^2 + p \\ \rho uv \\ \rho uw \\ \rho uE + up \\ \rho uz \\ \rho u\tau \end{pmatrix}, F^y = \begin{pmatrix} \rho v \\ \rho uv \\ \rho v^2 + p \\ \rho vw \\ \rho vE + vp \\ \rho vz \\ \rho v\tau \end{pmatrix}, F^z = \begin{pmatrix} \rho w \\ \rho uw \\ \rho vw \\ \rho w^2 + p \\ \rho wE + wp \\ \rho wz \\ \rho w\tau \end{pmatrix},$$

and

$$S = \begin{pmatrix} 0 \\ 0 \\ 0 \\ 0 \\ \kappa q_0 \rho z \\ -\kappa \rho z \\ -\rho \alpha \end{pmatrix}.$$

Here

$$E = e + \frac{1}{2}\rho u^2$$

and

$$p = (\gamma - 1)\rho e$$

where γ is the ratio of specifc heats, q_0 is the heat of reaction, α is the inverse induction time, and κ is the reaction rate.

There are three basic components to the numerical methodology we use to solve the above equations – the discretization strategy, representation of the geometry, and adaptive mesh refinement so that resolution can be selectively added and removed as the calculation progresses.

The basic discretization scheme is a higher order Godunov method. These methods have been very successful for high Mach-number flow, porous media flow, and when incorporated into a suitable projection formulation, for incompressible flows characterized by steep gradients. They can resolve detailed features of the solution without introducing excessie smearing or spurious oscillations.

In order to model the complex geometry of the pulse combustor, we use the Cartesian grid formulation of Pember *et al* (1993). In this formulation, the solid boundary is treated as a stationary tracked front in a regular Cartesian grid represented in a volume-of-fluid manner. By convention, volume fractions lying entirely within the flow domain are set to 1, those entirely within the body are set to zero and cells at the fluid-body interface are an appropriate fraction between zero and one (Figure 1).

The integration algorithm is a predictor-corrector formulation. In the predictor, we use a higher-order Godunov method to find a reference state in which the geometry is "ignored." In the corrector step, an adjustment at boundary cells is

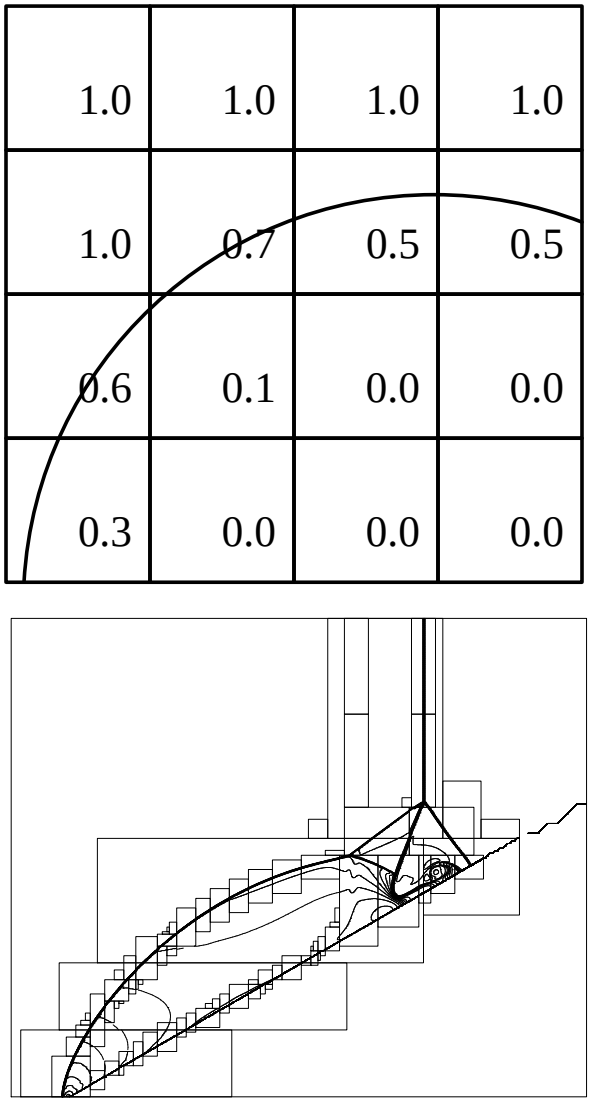

calculated. A redistribution procedure is applied to maintain conservation while avoiding time step restrictions arising from "small" cells.

The Godunov/Cartesian grid scheme is coupled to a local adaptive mesh refinement algorithm that selectively refines regions of the grid that require high resolution (Berger and Oliger, 1984; Berger and Colella, 1989; Bell *et al*, 1994). This procedure uses a hierachically nested sequence of logically rectangular grids upon which the solution is recursively calculated untuil the desired degree of acuracy is achieved. This proceudre has been highly effective in shock physics calculations, where steep gradients move through the flow domain, and has been shown to be one to two orders of magnitude more efficient than equivalent calculations on a uniform grid.

Further details of the adaptive Cartesian grid algorithm and its implementation can be found in Pember *et al.* (1993).

Modeling Issues

Limits on computer memory and time dictate that multidimensional reacting flow simulations walk a fine line of compromise between detailed modeling of the chemical kinetics and high-resolution treatment of the fluid dynamics. In this study, we assume pre-mixed combustion and use a simple, two equation kinetics model desribed by

$$\dot{\tau} = -\alpha$$

$$\dot{z} = \begin{cases} -\kappa z & \text{if } \tau < 0 \\ 0 & \text{otherwise} \end{cases}$$

$$z(0) = \tau(0) = 1$$

Here, z respresents the mass fraction of unburned material and τ is an advected "counter" that simulates an induction time; when it crosses zero, the fluid ignites. This enables us to easily "tune" the induction time to the acoustic transit time of the pressure waves in the duct.

The inlet valve in the combustion chamber is pressure-actuated – when the pressure goes below a certain threshold, it opens, allowing fuel and air to enter. The mixture ignites and the pressure in the chamber rises until the threshold is reached again. The valve closes and remains closed until the compression wave sent down the duct by the ignition arrives back in the combustion chamber as a rarefaction, dropping the chamber pressure again and beginning another cycle. Following Barr *et al.* 1990), we assume quasi-steady friction losses and derive the mass flow rate across the valve by conservation of momentum,

$$\frac{d}{dt}\dot{m} = \Delta p - C_f \dot{m},$$

with the restriction that

$$\dot{m} \geq 0.$$

The inlet velocity is calculated from the above o.d.e. when the pressure in the chamber at the location of the valve is less than one atmosphere. When the pressure rises above that threshold, reflecting wall boundary conditions are applied at the valve, "closing" it.

Since the flow in the duct is adequately described by the one-dimensional reacting gas dynamics equations, we instantiate a separate one-dimensional integration module for that region. The flow in the duct is coupled to the chamber via the boundary at the end of the converging region. Heat transfer and frictional losses in the duct are modeled by source terms in the conservation equations, as in Barr *et al.* (1990).

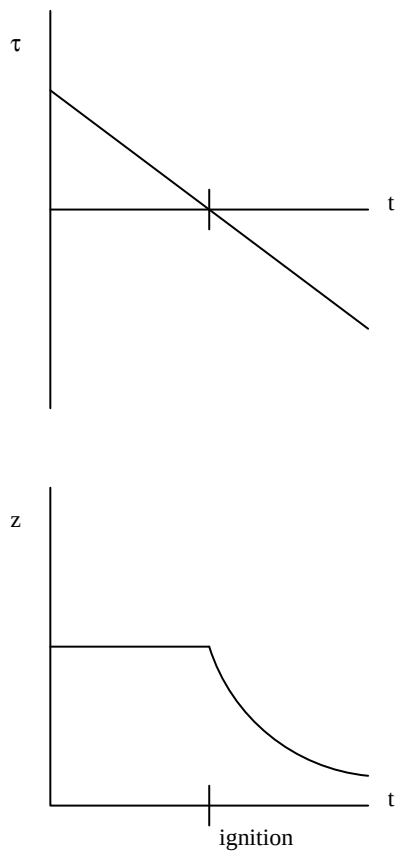
τ
t
z
t
ignition

In the momentum equation, we have

$$S_u = -\rho A \frac{4f}{D} \frac{u^2}{2} \frac{u}{\| u \|} \tag{2}$$

In the energy equation,

$$S_e = -4Dh(T - T_{amb}) \tag{3}$$

Implementation

This algorithm was implemented in a hybrid formualtion of C++ and Fortran. The former was used to for upper-level memory and data-structure management; the latter for low-level number crunching. Extensive class libraries have been written to support various "grid calculus" operations (Crutchfield and Welcome, 1994). This makes the problem of managing the hierarchical data structures of the AMR algorithm relatively straightforward. For this calculation in particular, the object-oriented nature of our approach greatly facilitated the implementation and coordination of the separate integrators for the duct and the combustion chamber.

Results

All calculations shown are for a methane-air fuel mixture, with a fractional N_2 dilution of 0.3.

The combustion chamber consists of a straight region followed by a tapering section leading to a long, narrow duct. Typically, the chamber is 20 cm. long by 10 cm. wide and the duct 200 cm. long by 3 cm. wide. As in some of the experimental configurations (Keller, 1993), a small baffle plate was placed in front of the valve opening to enhance mixing.

Table I : Parameter Values	
$R_c(J/kg - K)$, gas constant	$3.0078x10^6$
C_f, valve friction factor	$1.6847x10^4$
$q_0(J/s - m^3)$, energy release	$1.4x10^{10}$
$\kappa(s^{-1})$, rate of energy release	$2.8x10^6$
f, duct friction coefficient	0.01055
$h_c(W/m^2/K)$, comb. chamber heat transfer coeff.	17.92
$h_d(W/m^2/K)$, duct heat transfer coeff.	27.56
$A(cm^2)$, valve area	56.25
$\alpha(s^{-1})$, inverse induction time	200
$T_{ambient}$ (K)	300

Figure 4 shows the mass flow rate through the inlet valve as a function of time. The calculation was run for 81,000 time steps on a grid of 800 zones. It takes roughly half that time for a self-sustaining oscillation to establish itself. Figure 5 shows the

power spectral density of the mass flow rate for the first 41,000 steps; Figure 6 is a plot of the same quantity for the last 40,000 steps. In the latter plot, we observe a very clean spike at roughly 80 Hz, comparable to the experimentally observed frequency for similar conditions.

As Barr *et al.* (1990) have pointed out, success in attaining a self-sustaining pulsation is dependent on a variety of factors, among them, α, the inverse induction time. In the previous calculation, we set $\alpha = 200$. Figure 7 shows the mass flow rate for $\alpha = 20$, corresponding to an induction time of 50 ms. After 80,000 time steps, a clean pulsating combustion cycle still has not been established. Figure 8 shows the corresponding power spectrum. In Figures 9 and 10, we show the mass flow rate and power spectrum for $\alpha = 2000$, corresponding to almost immediate ignition. The broad-band power spectrum is suggestive of a chaotic regime. A more detailed analysis of the relationship between induction time, mass flow rate, and heat transfer in the duct will be the subject of a later study.

The quiescent state just prior to a new injection cycle (at time step 78,000 in the calculation shown in Figures 4 and 5) is used to initialize an axisymmetric calculation. Figures 11 and 12 show the mass flow rate and pressure at the valve for the first three cycles. The increased mass flow for the first cycle appears to be an artifact of the "bootstrap" procedure. In Figure 13, the combustion chamber is shown at four times during the cycle; pressure is shown on the left, mass fraction on the right. The ratcheting on the walls of the converging section is an artifact of the visualization, not the algorithm. The flow in the duct is not shown. The entrance jet begins to mushroom, strikes the stagnation plate, and diverges toward the walls. The fuel begins to burn, and the resulting rise in pressure closes the valve. After most of the remaining fuel is consumed, the incoming rarefaction from the duct opens the valve and the cycle begins again.

This calculation was run thorugh several complete cycles, and the data then used to initialize a prototypical three-dimensional calculation, shown in Figure 14. A base grid of 24x24x72 was used with one level of refinement at a factor of four, resulting in an equivelent single-grid resolution of 96x96x288 zones. In Figure 15, the mass flow rate of for the three-dimensional and axisymmetric calculations are compared. The total fuel injection in the three-dimensional case is slightly higher.

Conclusions

In this paper we have demonstrated the capability to carry out three-dimensional calculations of compressible, reacting flow in the complex engineering geometry of a pulse combustor. Ongoing work in this area includes incorporation of a multi-fluid flame capturing procedure into the scheme so that properties at the flame front can be more accurately calculated, implementation on parallel architectures, investigation of the dynamical systems aspects of the quasi-one-dimensional case, and detailed studies of three-dimensional vorticity dynamics of the reacting flow.

References

[1] P.K. Barr, J.O. Keller, T.T. Bramlette, C.K. Westbrook, and J.E.Dec (1990). Pulse combustor modeling: demonstration of the importance of characteristic times. *Combustion and Flame*, **82**,252-269.

[2] J. B. Bell, M. Berger, J. Saltzman, and M. Welcome (1994). Three dimensional adaptive mesh refinement for hyperbolic conservation laws. *SIAM J. Sci. Stat. Comput.* ,**15**(1), 127-138.

[3] M.J. Berger and P. Colella (1989). Local adaptive mesh refinement for shock hydrodynamics. *J. Comp. Phys.*, **82**, 64-84.

[4] M. J. Berger and J. Oliger (1984) Adaptive mesh refinement for hyperbolic partial differential equations. *J. Comp. Phys.*, **53**, 484-512.

[5] William Y. Crutchfield and Michael L. Welcome (1993). Object-oriented implementation of adaptive mesh refinement algorithms. *Scientific Programming*, **2**, 145-156.

[6] J.O. Keller, K. Saito (1987). Measurements of the comusting flow in a pulse combustor. *Combust. Sci. Tech.*. **53**, 137.

[7] J.O. Keller (1993). Private communication.

[8] J.O. Keller, T.T. Bramlette, C.K. Westbrook, and J.E.Dec (1989). Pulse combustor: the quantification of characteristic times. *Combustion and Flame*, **79**, 151.

[9] R.B. Pember, J.B. Bell, P. Colella, W.Y. Crutchfield, and M.L. Welcome (1993) Adaptive cartesian grid methods for representing geometry in inviscid, compressible flow. 11th AIAA Computational Fluid Dynamics Conference, Orlando, FL, July 6-9, 1993. *(submitted to J. Comp. Phys.)*

List of Figures

Figure 1. Schematic of fluid-body boundary intersecting grid in volume-of-fluid representation.

Figure 2. Application of hyperbolic AMR for inviscid compressible gas dynamics in interaction of shock and inclined ramp. Rectangles are grids used in the adaptive gridding strategy. Contours indicate changes of density.

Figure 3. Schematic of ignition time delay and kinetics models

Figure 4. Mass flow rate vs. time; $\alpha = 200$; 91,000 time steps.

Figure 5. Power spectrum of mass flow rate; $\alpha = 200$; first 41,000 time steps.

Figure 6. Power spectrum of mass flow rate; $\alpha = 200$; last 40,000 time steps.

Figure 7. Mass flow rate vs. time; $\alpha = 20$; 91,000 time steps.

Figure 8. Power spectrum of mass flow rate; $\alpha = 20$.

Figure 9. Mass flow rate vs. time; $\alpha = 2000$; 91,000 time steps.

Figure 10. Power spectrum of mass flow rate; $\alpha = 2000$.

Figure 11. Mass flow rate at valve for axisymmetric calculation.

Figure 12. Pressure signature at valve for axisymmetric calculation.

Figure 13. Pressure and density contours, axisymmetric calculation.

Figure 14. Single cycle of three-dimensional calculation, initialized from axisymmetric calculation.

Figure 15. Mass flow rate for single cycle of three-dimensional and axisymmetric calculations.